Conf-730705--1
RECEIVED BY TIC APR 24 1973

PHYSICS OF TARGET PLASMAS IN MINIMUM-B GEOMETRIES*

W. B. Ard, R. J. Colchin, E. C. Crume, J. L. Dunlap
G. R. Haste, N. H. Lazar, and J. F. Lyon

Oak Ridge National Laboratory
Oak Ridge, Tennessee, U.S.A.

This work with microwave-heated, hot-electron plasma is motivated by the expectation that such plasma can be developed to provide efficient targets for accumulation of a hot-ion plasma by energetic neutral injection. The intended application requires that the hot-electron plasma be established at low neutral gas density. These plasmas are unstable to flute modes at low pressure in simple magnetic mirror traps, and for this reason we have investigated properties of the plasma in magnetic well geometry.

We report experiments performed in the IMP facility, where superconducting mirror and quadrupole windings provide a variety of field configurations. The microwave sources have frequencies of 36 and 55 GHz. These are CW, each with a nominal power rating of 1 kW. The power at 36 GHz is used for resonant heating (resonant B = 12.5 kG) and that at 55 GHz for upper off-resonant heating. Our approach is to establish the plasma in a high mode cavity by application of the microwave power. Neutral density within the cavity is elevated above that of a surrounding vacuum chamber by a hydrogen gas leak. Plasma parameters are studied as a function of magnetic field configuration, H_2^0 density within the cavity, and microwave power levels. Principal diagnostics include ionization current flow out along field lines, free-free bremsstrahlung, diamagnetic pickup coils for total stored $W_\perp$, faster coils for monitoring rapid changes in $W_\perp$, injected fast H^0 beam, and calorimeters placed to measure plasma power to the walls.

Figure 1 shows a field configuration typical of those used in most of the experiments, which have involved resonant heating on closed magnetic surfaces. Indicated are the cavity outline, contours of constant $|B|$ (labeled by the ratio $|B|/B_0$), and field lines. Note that the contours with labels 1.1, 1.25, and 1.4 are the contours for the heating resonance with B_0 = 11.5, 10.0, and 9.0 kG, respectively.

Approximate radial profiles of $\int n_e d\ell$ can be obtained from the ionization current measurements. Examples are shown in Fig. 2 for the field configuration of Fig. 1. The experimental parameters ($n_0 = 10^{11}$ cm^{-3}, resonant power = 300

MASTER

*Research sponsored by the U.S. Atomic Energy Commission under contract with the Union Carbide Corporation.

watts, off-resonant power = 500 watts) are near optimum for plasma generated on such closed magnetic contours.

In the region near the z axis, the measurements yield hot-electron line densities $n_e d\ell \stackrel{\sim}{\sim} 5 \times 10^{12}$ cm^{-2}, where the line length between resonant contours on axis is $\sim$ 12 cm in the case B_0 = 10 kG. This density figure is confirmed by measurements of trapping out of a fast H^0 beam, and is also consistent with measurements of the total stored energy ($\stackrel{\sim}{\sim}$ 10-15 J), mean hot-electron energy (500-700 keV), and estimates of mean plasma volume (100 cm^3) based on the radial profiles. The expected distribution of plasma along the central field line suggests peak densities of $n_e = 1 \times 10^{12}$ cm^{-3}, so the highest ratio of plasma density to ambient neutral density (n_e/n_0) is about 10.

The radial profiles indicate a non-uniform filling of the available magnetic volume (that is, the volume within the $|B|$ contour for resonance). Possible explanations are that either the microwave power is not absorbed as efficiently at the larger radii, or the confinement of hot electrons is not as good in those regions. Since calorimetric measurements of power carried to the wall by the plasma show equal power density to be deposited in the plasma on and off axis, poor confinement is indicated.

Two mechanisms have been identified which can account for more rapid loss of energetic plasma in the outer regions: (a) non-adiabaticity of energetic electrons and (b) mirror instability caused by high anisotropy. Estimates of the effects of non-adiabaticity, based on the criterion that $1/\Omega^2 \, d\Omega/dt < C$, show electrons of energy greater than 4 MeV to be poorly confined even near the axis. The perpendicular field gradient increases with radius, and so confinement is expected to be poorer at larger radii. Anistropy of confined plasma, and hence the possibility of loss due to mirror instability, also increases with radius in these magnetic fields. The $|B|$ surface for resonant heating is also that for reflection of particles, so the mirroring field value does not vary with radius. However, the minimum field along flux lines increases with radius, and as a consequence the mirror ratio for confined particles approaches unity at the radial edge of the well. Plasma confined there is highly anisotropic and can become mirror unstable even at low β.

Evidence for non-adiabaticity is given in Fig. 3, which shows the electron distribution derived from bremsstrahlung data as a function of time in the plasma decay. The collimated line-of-sight was through the B_0 field point and was essentially in the median plane. The high energy cut-off for the steady state distribution is in good agreement with the calculated adiabatic limit for this central region. The most energetic electrons are observed to decay most rapidly in direct contradiction to the expected $\sim E^{3/2}$ dependence of lifetime. This rapid decay is presently interpreted as arising from classical scattering of these electrons into loss cones which are considerably larger for energetic electrons than for those of low energy. This "anomalous" loss cone arises from loss of adiabaticity of the very energetic particles as their parallel energy increases by scattering.

Signals which provide evidence for mirror instability (that is, a compression of the plasma configuration followed by a loss of stored energy) are observed with fast response magnetic pickup coils. Measurements of the power drain associated with these changes in stored energy indicate that the direct losses from this instability are much too low to effect the overall power balance. Although indirect effects on confinement (as, for example, electric fields leading to radial drift) are much more difficult to assess, our present feeling is that non-adiabaticity is the more dominant cause of poor confinement at larger radii.

The experiments detailed above dealt with plasma created by resonantly heating on a closed $|B|$ contour. We have also examined plasma in field configurations with less deep wells and the resonant contour an open one moved back into the coil throats. Only resonant power was available in such configurations. With this arrangement, the field lines linking the heating contours pass only through the central portion of the magnetic well. Stable plasma is formed with density comparable to that described above at significantly lower microwave power levels, with significantly higher n_e/n_0, more uniform radial profiles, and negligible power to a calorimeter just outside the column defined by the heating resonances. These observations reinforce our conclusion that plasma formed by resonance on closed magnetic contours exhibits poor confinement near the radial edges of the well. Further, since heating with the microwave fields did not cause drift of particles across surfaces of constant $J = \int p_z d\ell$ even with low $\partial J/\partial r$, the observations demonstrate that shallow magnetic well geometries can provide good confinement of these plasmas.

Figure Captions

Fig. 1 Cavity outline, magnetic field lines, and contours of constant $|B|$. The field properties are for a compensation ratio of 2.5, and for the plane between quadrupole "bars." The contours are labeled by the ratio of $|B|$ to B_0, the central field point; the field lines are labeled by the radius (in the z = 0 plane) of the $|B|$ contour for which $|B|$ equals the minimum B along the line.

Fig. 2 Ionization current as a function (radius) defined in Fig. 1. The currents plotted are initial amplitudes of the slowly decaying portion of the signal measured after shutting off the microwave power and are generally somewhat lower than steady-state levels.

Fig. 3 Electron energy distributions from free-free bremsstrahlung measurements. The figure gives the steady-state distribution and those obtained during successive time intervals after cutting off microwave power. The detector line-of-sight was through the B_0 fieldpoint at an inclination of 9° to the median (z = 0) plane, and so emphasizes the central portion of the plasma.

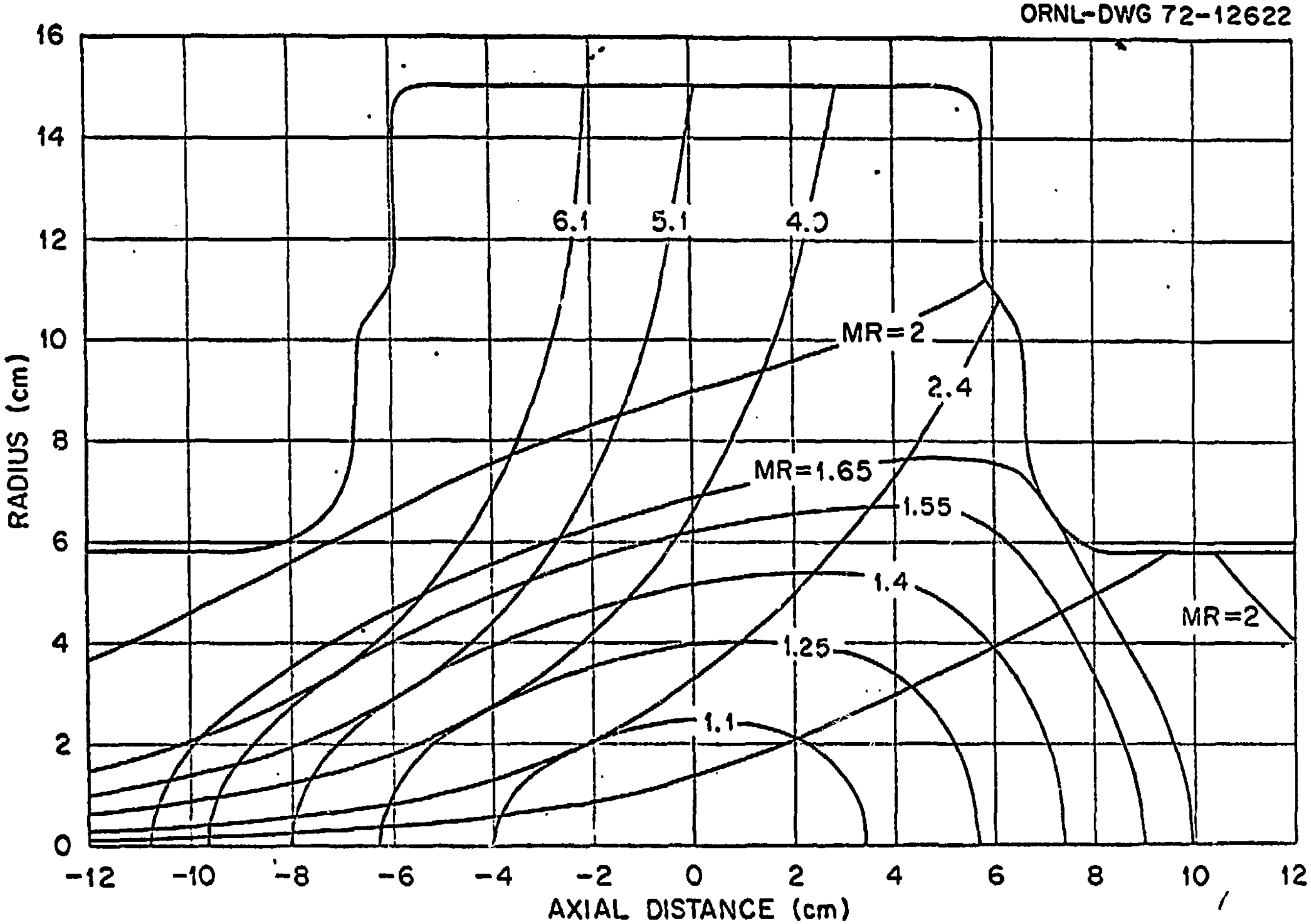

IMP: Field Lines and Contours, Symmetry Plane, CR=2.5.

FIGURE 1

FIGURE 2

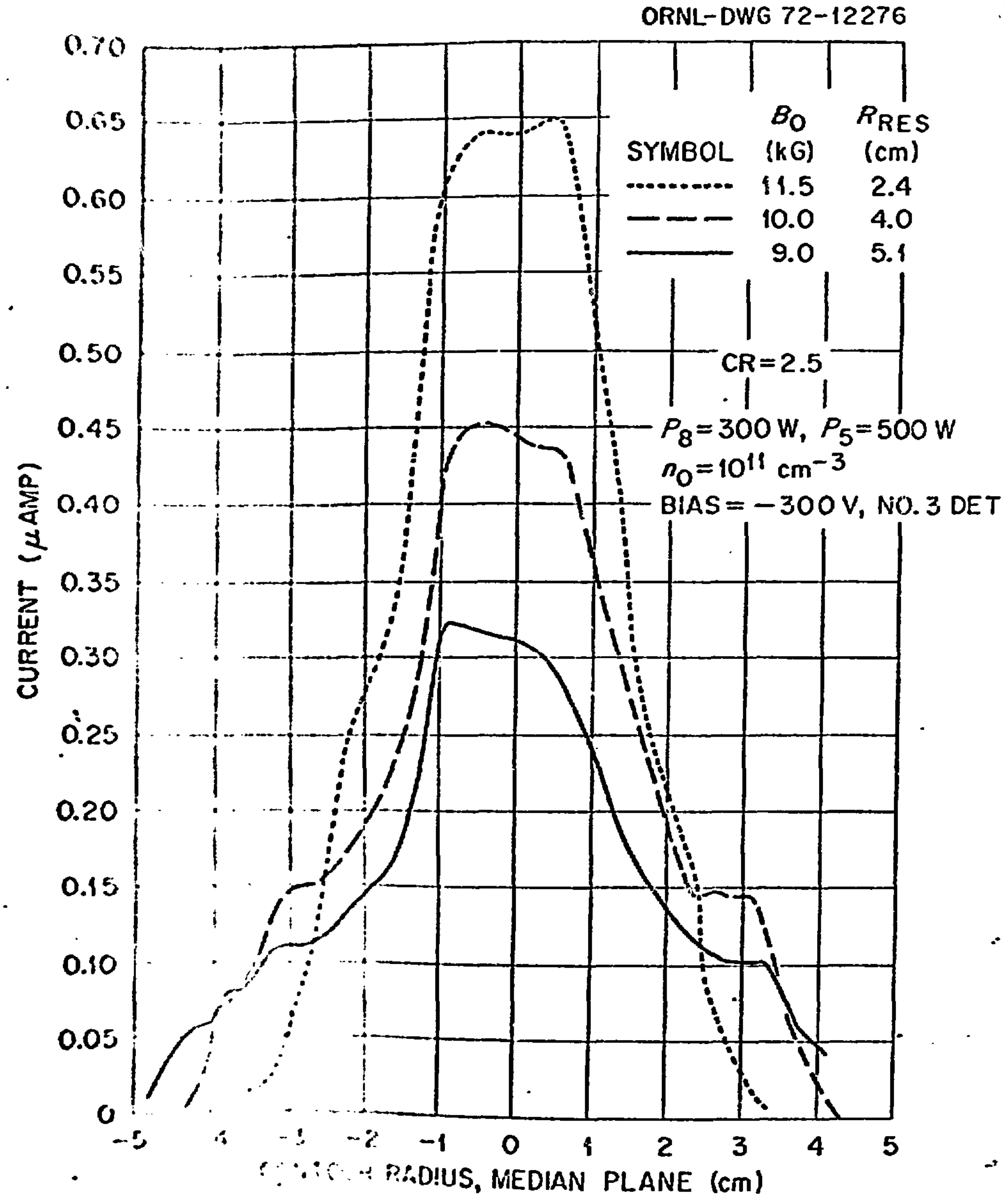

Ioniz[illegible] Studies, Initial Amplitude of Slow Decay Compon[illegible] 22, 25-72).

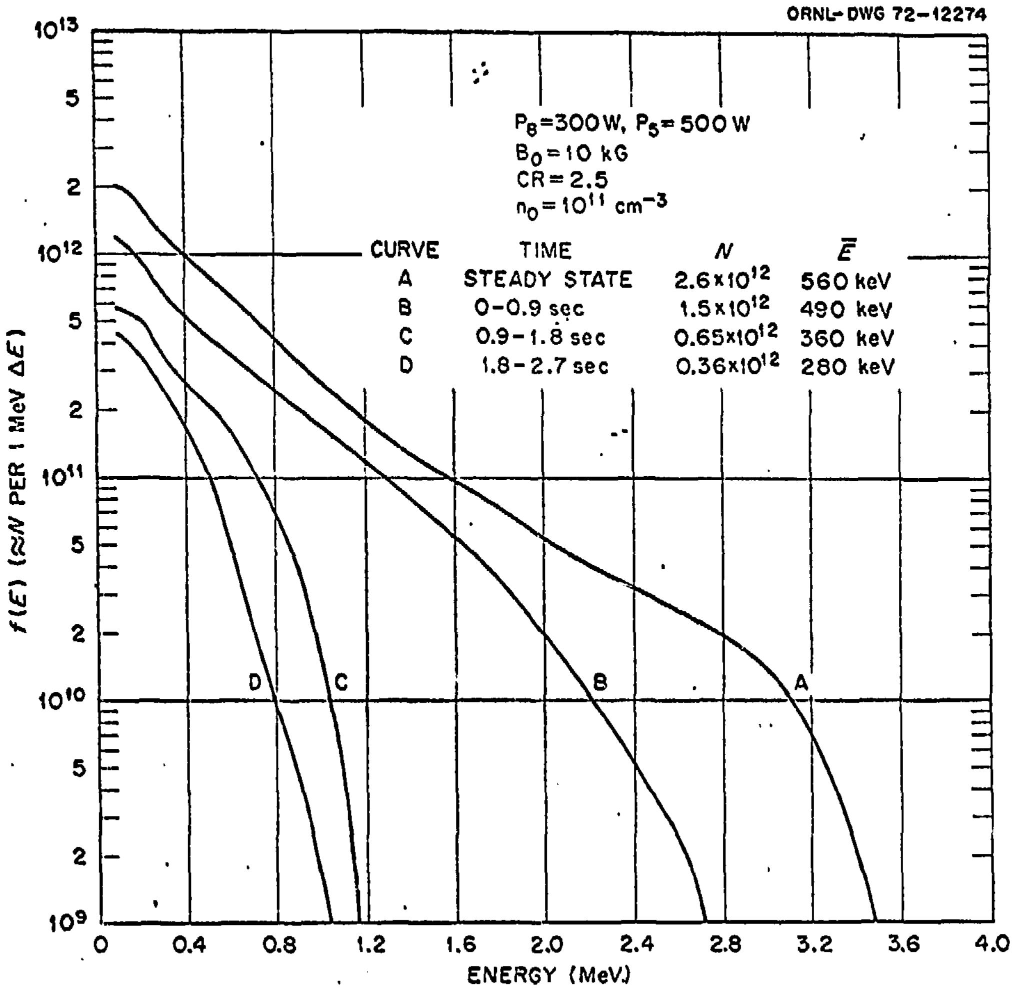

IMP: Electron Energy Distributions From Bremsstrahlung Measurements (Data 10/12/72).

FIGURE 3